

# Catalysis Science & Technology

Accepted Manuscript



This is an *Accepted Manuscript*, which has been through the Royal Society of Chemistry peer review process and has been accepted for publication.

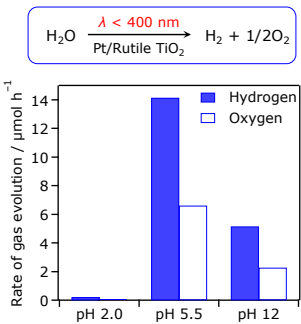
*Accepted Manuscripts* are published online shortly after acceptance, before technical editing, formatting and proof reading. Using this free service, authors can make their results available to the community, in citable form, before we publish the edited article. We will replace this *Accepted Manuscript* with the edited and formatted *Advance Article* as soon as it is available.

You can find more information about *Accepted Manuscripts* in the [Information for Authors](#).

Please note that technical editing may introduce minor changes to the text and/or graphics, which may alter content. The journal's standard [Terms & Conditions](#) and the [Ethical guidelines](#) still apply. In no event shall the Royal Society of Chemistry be held responsible for any errors or omissions in this *Accepted Manuscript* or any consequences arising from the use of any information it contains.

Graphical and textual abstract (GTA)

Graphical abstract



Textual abstract

Photocatalytic water-splitting activity of rutile TiO<sub>2</sub> was found to be very sensitive to the loaded cocatalyst and reaction pH.

## ARTICLE

Photocatalytic properties of rutile TiO<sub>2</sub> powder for overall water splitting

Cite this: DOI: 10.1039/x0xx00000x

Kazuhiko Maeda<sup>\*a,b</sup>Received 00th January 2012,  
Accepted 00th January 2012

DOI: 10.1039/x0xx00000x

www.rsc.org/

The application of illuminated rutile TiO<sub>2</sub> powder modified with a metal cocatalyst to overall water splitting generating H<sub>2</sub> and O<sub>2</sub> was studied. Although unmodified rutile exhibited little activity, modification with a suitable amount of Pt nanoparticles resulted in observable H<sub>2</sub> and O<sub>2</sub> evolution from pure water under band-gap irradiation. Pt-loaded rutile TiO<sub>2</sub> exhibited stable and high photocatalytic activity in pure water. The photocatalytic performance is much lower at acidic and basic condition, respectively, due to a photo-corrosion effect and inefficient water reduction process.

## 1. Introduction

Photocatalytic overall water splitting using an illuminated semiconductor particle is an important reaction from the viewpoint of light energy conversion to produce clean hydrogen.<sup>1</sup> So far, more than 100 semiconductor photocatalysts have been reported to exhibit water-splitting activity under band-gap irradiation, and most of them are metal oxides that have band gaps larger than 3.0 eV.<sup>1c,d</sup>

The present author very recently reported that rutile TiO<sub>2</sub> powder having a band gap of 3.0 eV is capable of splitting pure water into H<sub>2</sub> and O<sub>2</sub> under band-gap irradiation ( $\lambda < 400$  nm) without noticeable degradation.<sup>2</sup> Although the wavelength available for the reaction is limited to 400 nm, rutile TiO<sub>2</sub> is shown to be one of the smallest band-gap semiconductors among metal oxides that have been reported to achieve photocatalytic overall water splitting.

In general, water-splitting activity of a semiconductor photocatalyst is known to be strongly dependent both on the preparation conditions (e.g., cocatalysts) and the reaction conditions (e.g., pH).<sup>1g</sup> While many researchers have investigated these factors for various wide-gap metal oxide photocatalysts,<sup>3–8</sup> however, there are very few that report photocatalytic properties of a metal oxide having a band gap smaller than 3.0 eV for overall water splitting. Hence satisfactory knowledge on photocatalytic properties of such a medium gap metal oxide has yet to be obtained so far.

The present article reports on a more detailed investigation of the photocatalytic properties of rutile TiO<sub>2</sub> for overall water splitting with respect to cocatalyst-loading and reaction pH.

## 2. Experimental

2.1. Preparation of rutile TiO<sub>2</sub>

TiO<sub>2</sub> powder containing rutile as the main phase was supplied by the Toho Titanium Co. (sample HT0210). This sample has previously been reported to exhibit very high photocatalytic

activity for water oxidation half reaction in the presence of IO<sub>3</sub><sup>–</sup> ions as an electron acceptor under UV irradiation.<sup>9</sup> It was heated at 1273 K for 2 h in air to convert residual anatase phase into rutile. The calcined sample is referred to hereafter as R-TiO<sub>2</sub>.

## 2.2. Modification with cocatalysts

Modification of R-TiO<sub>2</sub> with nanoparticulate metal cocatalysts was accomplished by an in-situ photodeposition method, in which metal nanoparticles are deposited at reduction sites on a semiconductor photocatalyst.<sup>10</sup> Photodeposition was carried out in a closed gas circulation system made of glass, similar to the photocatalytic reaction system described below. The powdered R-TiO<sub>2</sub> was first dispersed in pure water (100 mL) containing an appropriate amount of the metal source, using a magnetic stirrer. In the present study, (NH<sub>4</sub>)<sub>2</sub>RuCl<sub>6</sub> (Aldrich), Na<sub>3</sub>RhCl<sub>6</sub>·*n*H<sub>2</sub>O (Mitsuwa Chemicals, 17.8% Rh), (NH<sub>4</sub>)<sub>2</sub>PdCl<sub>4</sub> (Kanto Chemicals, 37% Pd), Na<sub>2</sub>IrCl<sub>6</sub>·6H<sub>2</sub>O (Kanto Chemicals, 97% Ir), H<sub>2</sub>PtCl<sub>6</sub>·2H<sub>2</sub>O (Kanto Chemicals, 97% Pt) and HAuCl<sub>4</sub>·4H<sub>2</sub>O (Kanto Chemicals, 99.0%) were used as cocatalyst precursors without further purification. After mixing, each solution was evacuated to completely remove dissolved air and then irradiated with UV light ( $\lambda > 350$  nm) for 4 h. Following filtration and washing with pure water the resulting powder was dried in an electric furnace at 473 K for 1 h.

To demonstrate the presence of oxidation sites on R-TiO<sub>2</sub>, the photodeposition of PbO<sub>2</sub> was also performed, using Pb(NO<sub>3</sub>)<sub>2</sub> (Wako Pure Chemicals, 99.9%) as the precursor in an aqueous HNO<sub>3</sub> solution (pH = 1) under aerated conditions according to the method of Matsumoto et al.<sup>11</sup> The irradiation conditions applied were similar to those used during the photodeposition of the other metals, as described above.

## 2.3. Structural characterization

The rutile TiO<sub>2</sub> samples were characterized by X-ray diffraction (XRD; MiniFlex 600, Rigaku), UV-visible

spectrometer (UV-vis. DRS; V-565, Jasco) and scanning electron microscopy (SEM; S-4700, Hitachi). The Brunauer-Emmett-Teller (BET) surface areas of R-TiO<sub>2</sub> was measured, using a BELSORP-mini apparatus (BEL Japan) at liquid nitrogen temperature (77 K).

#### 2.4. Water splitting reactions

Reactions were conducted in a Pyrex top-irradiation vessel connected to a glass closed gas circulation system. A 100 mg sample of metal-deposited R-TiO<sub>2</sub> powder was dispersed in pure water (100 mL) using a magnetic stirrer and this reactant solution was evacuated under vacuum several times to completely remove any residual air, following which a small amount of Ar gas (ca. 5 kPa) was introduced into the reaction system prior to irradiation under a 300 W xenon lamp (Cermex, PE300BF) with a 20 A output current. The irradiation wavelength was controlled by a cold mirror and water filter ( $\lambda > 350$  nm) and the reactant solution was maintained at room temperature by a water bath during the reaction. The evolved gases were analysed by gas chromatography (Shimadzu, GC-8A with TCD detector and MS-5A column, argon carrier gas).

#### 2.5. Photoelectrochemical measurements

Porous electrodes made of R-TiO<sub>2</sub> were prepared by pasting a viscous slurry onto conductive glass according to a previously described method, with some modifications.<sup>12</sup> A mixture of 50 mg of R-TiO<sub>2</sub> powder, 10  $\mu$ L of acetyl acetone (Kanto Chemicals), 10  $\mu$ L of Triton X (Aldrich, USA), 10  $\mu$ L of poly(ethylene glycol) 300 (Kanto Chemicals) and 500  $\mu$ L of distilled water was ground in an agate mortar to prepare the viscous slurry. The slurry was then pasted onto fluorine-doped tin oxide (FTO) glass slides (thickness 1.8 mm; Asahi Glass, Japan) to prepare 1.5 $\times$ 3.5 cm<sup>2</sup> electrodes, which were subsequently calcined in air at 723 K for 1 h.

Photoelectrochemical measurements were carried out using a potentiostat (HSV-110, Hokuto Denko) and an electrochemical cell at room temperature. The cell was made of Pyrex glass and consisted of a three electrode-type system using Pt wire and an Ag/AgCl electrode as the counter and reference electrodes, respectively. An aqueous Na<sub>2</sub>SO<sub>4</sub> solution (pH = 5.9 or 12) was employed as the electrolyte and was saturated with argon gas prior to the electrochemical measurements. The light source was a xenon lamp (300 W) fitted with a cold mirror ( $\lambda > 350$  nm). The potential of the photoelectrode was reported against the reversible hydrogen electrode (RHE) as follows.

$$E_{\text{RHE}} = E_{\text{AgCl}} + 0.059 \text{ pH} + E^{\circ}_{\text{AgCl}} \quad (E^{\circ}_{\text{AgCl}} = 0.1976 \text{ V at 298 K})$$

### 3. Results and discussion

#### 3.1. Physicochemical characterization

Fig. 1A shows the XRD pattern of R-TiO<sub>2</sub>, along with the data for the original HT0210. R-TiO<sub>2</sub> exhibited a single-phase diffraction pattern assigned to rutile. Calcination at temperatures lower than 1273 K evidently failed to convert the residual anatase phase to rutile (data not shown here). UV-visible diffuse reflectance spectroscopy indicated that R-TiO<sub>2</sub> has a steep absorption edge at 400 nm, corresponding to a 3.0 eV band gap (Fig. 1B). As can be seen from Fig. 1C, R-TiO<sub>2</sub> was composed of well-crystallized particles ranging in size from several hundred nanometers to 1–2 micrometers. It is also evident that the R-TiO<sub>2</sub> contained exposed crystal faces with surface nanostep structures. The specific surface area, as determined by nitrogen adsorption at 77 K, was 1.4 m<sup>2</sup> g<sup>-1</sup>.

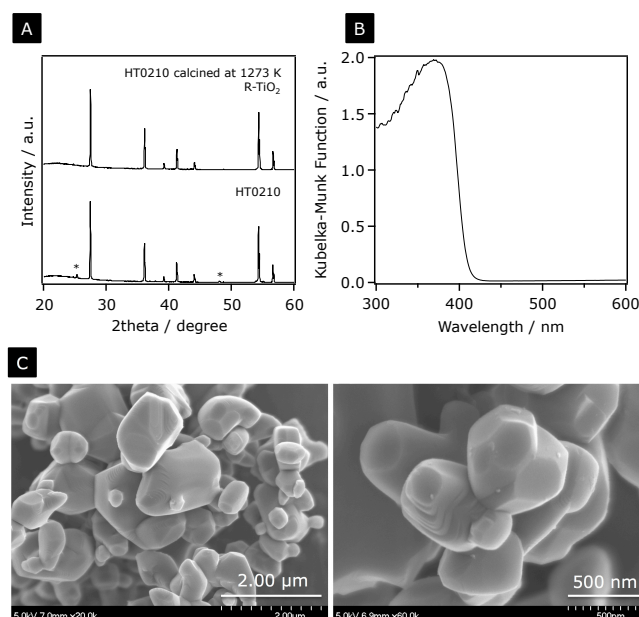


Fig. 1 (A) XRD pattern, (B) UV-visible diffuse reflectance spectrum, and (C) SEM images of R-TiO<sub>2</sub>. \* in the panel (A) indicates diffraction peaks assigned to anatase TiO<sub>2</sub>.

#### 3.2. Effect of modification of R-TiO<sub>2</sub> with metal cocatalysts on water splitting activity

It is known that the photocatalytic activity of a given semiconductor for overall water splitting is strongly dependent on the presence of a cocatalyst<sup>1g</sup> and thus the effects of the cocatalyst loading of rutile TiO<sub>2</sub> on water splitting activity were examined. Table 1 presents the rates of H<sub>2</sub> and O<sub>2</sub> evolution from pure water using R-TiO<sub>2</sub> modified with various metal cocatalysts. Simultaneous H<sub>2</sub> and O<sub>2</sub> evolution from pure water was observed when Rh, Pd or Pt were employed, while Ru, Ir and Au did not show any promotion of the catalysis. A mixed oxide of Rh and Cr, which has been reported to be effective as a cocatalyst for many semiconductor photocatalysts,<sup>13</sup> did not work as well (data not shown here).

**Table 1.** Effect of modification of R-TiO<sub>2</sub> with various metal cocatalysts on water splitting<sup>a</sup>

Entry	Cocatalyst	Loading amount / wt%	Amount of products for 4 h / $\mu$ mol	
			H <sub>2</sub>	O <sub>2</sub>
1	None	0	0	0
2	Ru	0.1	0	0
3	Rh	0.1	2.5	0.9
4	Pd	0.1	3.7	0.9
5	Ir	0.1	0	0
6	Pt	0.1	56.6	26.5
7	Au	0.1	0	0
8	Pt	0.01	21.6	9.4
9	Pt	0.05	35.5	13.8
10	Pt	0.5	23.2	9.7
11	Pt	1.0	5.6	2.8

<sup>a</sup> Reaction conditions: catalyst, 100 mg (cocatalyst-loaded); pure water, 100 mL, xenon lamp (300 W) fitted with a cold mirror (CM-1); reaction vessel, Pyrex top-irradiation type.

Because Pt was found to be the most effective cocatalyst among those examined (entry 6), the effect of the amount of Pt loaded on the rutile sample was investigated in more detail. While the unmodified sample did not show activity, loading just 0.01 wt% of Pt resulted in clearly observable  $\text{H}_2$  and  $\text{O}_2$  evolution in a nearly stoichiometric ratio ( $\text{H}_2/\text{O}_2 \approx 2$ ). With increasing Pt loading, the rates of both  $\text{H}_2$  and  $\text{O}_2$  evolution increased, reaching a maximum at 0.1 wt%, then decreasing (Table 1, entries 6, 8–11). The slight deviation of the  $\text{H}_2/\text{O}_2$  ratio from the ideal stoichiometric value was due to the photoreduction of  $\text{O}_2$  via a reverse reaction during water splitting, as has already been discussed in the previous work.<sup>2</sup> The previous study also confirmed that Pt-loaded rutile  $\text{TiO}_2$  exhibits stable performance for pure water splitting without any noticeable change in its photocatalyst structure.<sup>2</sup>

### 3.3 Behaviour of Pt photodeposition on rutile $\text{TiO}_2$

The deposited Pt nanoparticles were observed by means of SEM. As shown in Fig. 2, well-dispersed Pt nanoparticles were observed despite the relatively large amount of Pt which had been added (1.0 wt%). It is important to stress that the Pt nanoparticles did not undergo photodeposition on certain crystal faces, including the nanostep structures, suggesting that these surfaces were not available for reduction reactions.

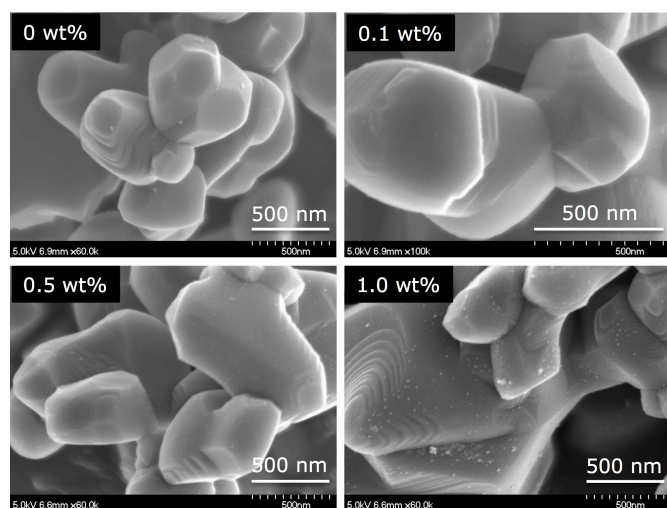


Fig. 2 SEM images of R- $\text{TiO}_2$  loaded with different amount of Pt.

The nature of the active sites on R- $\text{TiO}_2$  was further examined by conducting photodeposition of  $\text{PbO}_2$  onto a 0.1 wt% Pt-loaded sample. Fig. 3 shows SEM images of the resulting  $\text{PbO}_2$ -deposited sample in which  $\text{PbO}_2$  deposits are clearly distinguishable as aggregated 30–50 nm particles. In contrast to the relatively highly dispersed, reductively photodeposited Pt nanoparticles (Fig. 2), the aggregated  $\text{PbO}_2$  particles were assembled only at certain surfaces. In particular, preferential deposition of  $\text{PbO}_2$  on the nanostep structures can be seen, suggesting that oxidation sites were narrowly distributed on the R- $\text{TiO}_2$  surface and were situated preferentially on (or near) the nanostep structures. The reduction and oxidation sites were therefore separated in R- $\text{TiO}_2$  since they occurred on different crystal faces.

Ohno et al. previously studied reduction and oxidation reaction sites on rutile  $\text{TiO}_2$  with exposed crystal faces<sup>14</sup> and

determined that  $[\text{PtCl}_6]^{2-}$  ions were reduced to Pt nanoparticles and deposited on the {110} face of the rutile  $\text{TiO}_2$  particles, while  $\text{PbO}_2$  generated by the oxidation of  $\text{Pb}^{2+}$  ions was found on the surface of the {011} face. Unfortunately, during the present study, it was difficult to assign the crystal faces in R- $\text{TiO}_2$  because the crystal habit could not be determined with certainty (Fig. 1C).

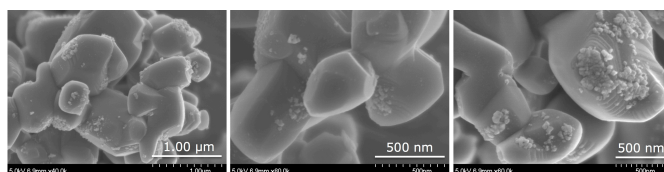


Fig. 3 SEM images of R- $\text{TiO}_2$ , further photodeposited with 2.4 wt %  $\text{PbO}_2$ .

### 3.4. Effect of reaction pH on activity

Fig. 4 shows the time courses of overall water splitting under UV irradiation ( $\lambda > 350$  nm) on 0.1 wt% Pt-loaded R- $\text{TiO}_2$  at various pH values. At pH 2.0, the photocatalyst exhibited the lowest activity among the series of reactions, producing only  $\text{H}_2$ . Basic reaction condition (pH 12) was also not very suitable for overall water splitting. The highest performance was obtained at pH 5.5 (without any pH control). Although the rates of  $\text{H}_2$  and  $\text{O}_2$  evolution decreased markedly as the reaction proceeded due to  $\text{H}_2$ – $\text{O}_2$  recombination on the loaded Pt nanoparticles and photo-reduction of  $\text{O}_2$ , the previous study revealed that this is a “reversible” deactivation, and the photocatalytic system itself is stable.<sup>2,15</sup> It should be also noted that as reported in the previous study,<sup>2</sup> the water-splitting rate recorded during an in-situ Pt-photodeposition condition (pure water with a small amount of  $\text{H}_2\text{PtCl}_6$ ) was lower than that achieved in the present study (pure water only). This is due primarily to the generation of protons under the photodeposition condition, which results from the consumption of the  $\text{H}_2\text{PtCl}_6$  precursor. This is consistent with the present result, which indicated that the performance of Pt-loaded R- $\text{TiO}_2$  was very low in acidic pH.

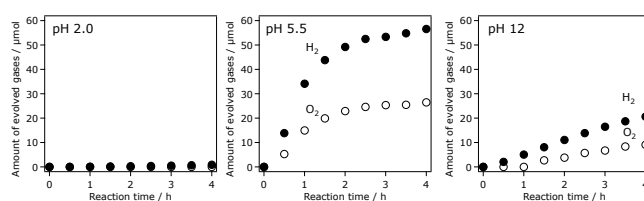


Fig. 4 Time courses of water splitting using 0.1 wt% Pt-loaded R- $\text{TiO}_2$  at different pH conditions. Reaction conditions: catalyst, 100 mg; aqueous solution, 100 mL, xenon lamp (300 W) fitted with a cold mirror (CM-1); reaction vessel, Pyrex top-irradiation type. Closed circles,  $\text{H}_2$ ; open circles,  $\text{O}_2$ .

### 3.5. Factors affecting the water splitting activity of rutile $\text{TiO}_2$

The results of water splitting reactions (Table 1) indicated that loading an optimal amount of Pt nanoparticles is essential to enhancing the reaction rate. It is known that Pt is capable of acting as an excellent catalyst for  $\text{H}_2$  evolution, since it has the smallest overvoltage among the metals.<sup>16</sup> As a result, it appears that the water splitting rate obtained from rutile  $\text{TiO}_2$  is related to the overvoltage of the metals for  $\text{H}_2$  evolution, although



other factors cannot be excluded. Teratani et al. have reported that the rate of  $H_2$  evolution from an aqueous 2-propanol solution using an anatase  $TiO_2$  sample was dependent on the loaded metal, and that Pt was the most effective cocatalyst among the metals examined.<sup>17</sup>

As can be seen from Table 1, there is a definite structure to the relationship between Pt loading and activity; enhancement of the activity occurred from 0 to 0.1 wt% Pt loading, attributed to an increase in the density of active sites for  $H_2$  evolution, followed by decreasing activity with higher Pt loading due to excess coverage of the rutile sample by Pt nanoparticles.<sup>18</sup> The gray coloration of the Pt-loaded samples was observed to darken with increasing Pt loading, primarily due to such excess coverage. Excess Pt loading can potentially cause an inner-filter effect, thereby contributing to a decrease in activity and this is supported by the results of SEM observations. As shown in Fig. 2, Pt nanoparticles smaller than 10 nm were dispersed over the 0.1 wt% loading sample, which exhibited the highest activity. previous TEM observations have revealed that, in addition to ~10 nm nanoparticles, there were even smaller Pt nanoparticles present on the samples, approximately 2 nm in size.<sup>2</sup> As the loading amount of Pt was increased, the surface of the R- $TiO_2$  underwent more coverage and the size of the Pt deposits increased.

Although it has been confirmed by the previous study that rutile  $TiO_2$  achieves the functionality as a stable photocatalyst to split water into  $H_2$  and  $O_2$  at neutral pH,<sup>2</sup> the results of photocatalytic reactions at different pH conditions indicated that the performance of R- $TiO_2$  for overall water splitting is much lower at acidic pH (Fig. 4). It is known that rutile  $TiO_2$  undergoes anodic photo-corrosion, which competes with water oxidation, in an aqueous  $H_2SO_4$  solution when employed as a photoanode for water oxidation.<sup>18</sup> Therefore, the low activity at acidic pH condition can be explained reasonably in terms of the anodic photo-corrosion effect.

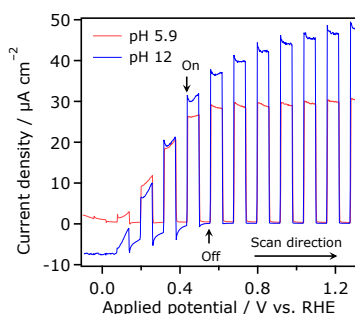


Fig. 5 Current-voltage curves obtained with R- $TiO_2$  electrodes ( $5.25\text{ cm}^2$ ) in aqueous 0.1 M  $Na_2SO_4$  solution (pH = 5.9 and 12 (adjusted by NaOH)) under intermittent UV irradiation ( $\lambda > 350\text{ nm}$ ). Scan rate:  $20\text{ mV s}^{-1}$ .

With increasing pH from 5.5 (in pure water), the photocatalytic performance decreased (Fig. 4). This characteristic pH dependence of the Pt-loaded R- $TiO_2$  photocatalyst deviates from the general character of transition metal oxide-based photocatalysts. For example, NiO/Sr $TiO_3$  and NiO/NaTaO<sub>3</sub> photocatalysts favour alkaline solutions for overall water splitting.<sup>3,7,8</sup> To investigate the water oxidation behaviour, photoelectrochemical measurements were conducted using a porous rutile  $TiO_2$  electrode. As shown in Fig. 5, the anodic photoresponse, which is characteristic to an n-type semiconductor, was a little better at pH 12 (in an aqueous NaOH solution) than at pH 5.9 (in an aqueous  $Na_2SO_4$  solution without any pH adjustment), indicating that increasing pH from

5.9 to 12 has a positive impact on water oxidation to some extent. A plausible explanation for the observed drop in activity from neutral to basic condition is that the water reduction process is hindered with increasing pH. At basic reaction conditions, the concentration of protons is of course lower than at neutral or acidic conditions. The decrease in proton concentration would hinder the water reduction process that occurs on Pt-loaded R- $TiO_2$ . Because the conduction band minimum of rutile  $TiO_2$  is located just above the  $H^+/H_2$  redox potential (in other words, the driving force for water reduction is low),<sup>19</sup> a decrease in the concentration of protons appears to be a critical factor that determines the overall efficiency, different from wide-gap metal oxide photocatalysts that have been reported to be active for overall water splitting. This idea is also supported by the result of photocatalytic reactions using different metal cocatalysts, which indicated that Pt, which has the lowest overvoltage for  $H_2$  evolution, exhibited the highest performance as a cocatalyst (Table 1).

Because of these two conflicting factors (anodic photo-corrosion at acidic pH and slow water reduction at basic pH), neutral pH condition is concluded to be suitable for overall water splitting by rutile  $TiO_2$ . Although rutile  $TiO_2$  is classified as d<sup>0</sup>-type photocatalysts like Sr $TiO_3$  and NaTaO<sub>3</sub>, facilitating the water reduction process appear to be more important due to the relatively low water reduction ability, reflecting the unique photocatalytic properties of rutile  $TiO_2$  for overall water splitting.

#### 4. Conclusions

The photocatalytic activity of rutile  $TiO_2$  for overall water splitting was investigated with respect to cocatalyst-loading and reaction pH. Among metal cocatalysts examined, Pt was found to be most suitable for the reaction. Pt-loaded rutile  $TiO_2$  was shown to be most stable in pure water at neutral reaction pH. The photocatalytic performance was lower at acidic and basic environment, attributable to anodic photo-corrosion in the catalyst and slow water reduction, respectively. This study highlighted that facilitating the water reduction process while suppressing anodic photo-corrosion contributes to higher performance for overall water splitting by rutile  $TiO_2$ .

#### Acknowledgements

The author would like to thank Professors Takashi Hisatomi and Kazunari Domen (The University of Tokyo) for assistance in SEM observations. This work was supported by the PRESTO/JST program "Chemical Conversion of Light Energy" and a Grant-in-Aid for Young Scientists (A) (Project No. 25709078). The author also thanks the Toho Titanium Co. for supplying a  $TiO_2$  sample.

#### Notes and references

- <sup>a</sup> Department of Chemistry, Graduate School of Science and Engineering, Tokyo Institute of Technology, 2-12-1-NE-2 Ookayama, Meguro-ku, Tokyo 152-8550, Japan.
- <sup>b</sup> Precursory Research for Embryonic Science and Technology (PRESTO), Japan Science and Technology Agency (JST), 4-1-8 Honcho Kawaguchi, Saitama 332-0012, Japan.
1. (a) A. J. Bard and M. A. Fox, *Acc. Chem. Res.*, 1995, **28**, 141; (b) K. Maeda and K. Domen, *J. Phys. Chem. C*, 2007, **111**, 7851; (c) F. E. Osterloh, *Chem. Mater.*, 2008, **20**, 35; (d) Y. Miseki and A. Kudo, *Chem. Soc. Rev.*, 2009, **38**, 235; (e) W. J. Youngblood, S.-H. A.

- Lee, K. Maeda, T. E. Mallouk, *Acc. Chem. Res.*, 2009, **42**, 1966;  
(f) R. Abe, *J. Photochem. Photobiol. C*, 2010, **11**, 179; (g) K.  
Maeda, *J. Photochem. Photobiol. C*, 2011, **12**, 237.
2. K. Maeda, *Chem. Commun.*, 2013, **49**, 8404.
3. K. Domen, S. Naito, T. Onishi and K. Tamaru, *Chem. Phys. Lett.*,  
1982, **92**, 433.
4. A. Kudo, A. Tanaka, K. Domen, K. Maruya, K. Aika and T. Onishi, *J.*  
*Catal.*, 1988, **111**, 67.
5. T. Takata, K. Shinohara, A. Tanaka, M. Hara, J. N. Kondo and K.  
Domen, *J. Photochem. Photobiol. A: Chem.*, 1997, **106**, 45.
6. D. W. Hwang, H. G. Kim, J. Kim, K. Y. Cha, Y. G. Kim and J. S.  
Lee, *J. Catal.*, 2000, **193**, 40.
7. H. Kato and A. Kudo, *J. Phys. Chem. B*, 2001, **105**, 4285.
8. H. Kato, K. Asakura and A. Kudo, *J. Am. Chem. Soc.*, 2003, **125**,  
3082.
9. R. Abe, K. Sayama and H. Sugihara, *J. Phys. Chem. B*, 2005, **109**,  
16052.
10. B. Kraeutler and A. J. Bard, *J. Am. Chem. Soc.*, 1978, **100**, 4317.
11. Y. Matsumoto, M. Noguchi and T. Matsunaga, *J. Phys. Chem. B*,  
1999, **103**, 7190.
12. R. Abe, T. Takata, H. Sugihara and K. Domen, *Chem. Lett.*, 2005, **34**,  
1162.
13. (a) K. Maeda, K. Teramura, D. Lu, T. Takata, N. Saito, Y. Inoue and  
K. Domen, *Nature*, 2006, **440**, 295; (b) K. Maeda, K. Teramura, D.  
Lu, T. Takata, N. Saito, Y. Inoue and K. Domen, *J. Phys. Chem. B*,  
2006, **110**, 13753; (c) K. Maeda, K. Teramura, N. Saito, Y. Inoue  
and K. Domen, *J. Catal.*, 2006, **243**, 303.
14. T. Ohno, K. Sarukawa and M. Matsumura, *New J. Chem.*, 2002, **22**,  
1167.
15. The result of recyclability of Pt-loaded rutile TiO<sub>2</sub> for overall water  
splitting can be found in ESI of the ref. 2.
16. J. O. Bockris and D. M. Drazic, *Electro-Chemical Science*; Taylor  
and Francis: London, 1972.
17. S. Teratani, J. Nakamichi, K. Taya and K. Tanaka, *Bull. Chem. Soc.*  
*Jpn.*, 1982, **55**, 1688.
18. P. Salvador, *Progress in Surf. Sci.*, 2011, **86**, 41.
19. L. Kavan, M. Grätzel, S. E. Gilbert, C. Klemenz and H. J. Scheel, *J.*  
*Am. Chem. Soc.*, 1996, **118**, 6716.